

Cedar Lake, Wisconsin - Limnological response to alum treatment: 2017 interim report

28 January, 2018



University of Wisconsin – Stout
Sustainability Sciences Institute - Center for
Limnological Research and Rehabilitation
Department of Biology
123E Jarvis Hall
Menomonie, Wisconsin 54751
715-338-4395
jamesw@uwstout.edu



Harmony Environmental
516 Keller Ave S
Amery, Wisconsin 54001
715-268-9992
harmonyenv@amerytel.net

Objective

Multiple Al applications over a period of 12 years are planned for Cedar Lake in order to control internal phosphorus loading. It is critical to conduct post-treatment monitoring of water and sediment chemistry to document the trajectory of water quality improvement during rehabilitation to make informed decisions regarding adjusting management to meet future water quality goals. Post-treatment monitoring included field and laboratory research to document changes in 1) hydrology and watershed phosphorus loading, 2) the phosphorus budget and lake water quality, 3) binding of sediment mobile phosphorus fractions that have contributed to internal phosphorus loading by alum, and 4) rates of diffusive phosphorus flux from the sediment under anaerobic conditions. Overall, lake water quality is predicted to respond to watershed and internal phosphorus loading reduction with lower total phosphorus and chlorophyll concentrations throughout the summer, lower bloom frequency of nuisance chlorophyll levels, and higher water transparency. Multiple Al applications between 2017 and 2029 should result in the binding of iron-bound phosphorus and substantial reduction in diffusive phosphorus flux from sediments under anaerobic conditions (i.e., internal phosphorus loading).

Methods

Watershed loading and lake monitoring

A gauging station was established on Horse Creek above Cedar Lake at 10th Ave for concentration, loading, and flow determination between April and October 2017 (Fig. 1). Grab samples were collected biweekly at the 10th Ave gauging station for chemical analysis. Water samples were analyzed for TSS, total phosphorus, and soluble reactive phosphorus using standard methods (APHA 2011, Wisconsin State Lab of Hygiene). Summer tributary phosphorus loading was calculated using the computer program FLUX.

The deep basin water quality station WQ 2 was sampled biweekly between May and October 2017 (Fig. 1). An integrated sample over the upper 2-m was collected for analysis of total phosphorus, soluble reactive phosphorus, and chlorophyll a. An additional discrete sample was

collected within 0.5 m of the sediment surface for analysis of total and soluble reactive P. Secchi transparency and in situ measurements (temperature, dissolved oxygen, pH, and conductivity) were collected on each date using a YSI 6600 sonde (Yellow Springs Instruments) that was calibrated against dissolved oxygen Winkler titrations (APHA 2011) and known buffer solutions.

The year 2010 was used in pretreatment (2010) versus post-treatment (2017) comparisons to evaluate the effectiveness of the alum treatment in improving limnological conditions. The summer of 2010 exhibited similar stratification patterns as 2017 and the duration of bottom anoxia was similar during both years allowing for better comparisons of changes in hypolimnetic P concentrations under anoxic conditions and chlorophyll response to internal P loading during the Fall mixing period. The year 2009 exhibited multiple periods of summer mixing and complete turnover, making comparisons with the post-treatment year 2017 more complex.

Sediment chemistry

Vertical variations. A sediment core was collected on 1 June (i.e., prior to alum treatment) and 23 August (i.e., ~ 1.5 months after alum treatment) 2017 at WQ 2 for determination of vertical profiles of various sediment characteristics and phosphorus fractions (see Analytical methods below). Sediment cores were sectioned at 1-cm intervals between 0 and 10 cm and at 2-cm intervals below the 10-cm depth for determination of moisture content, wet and dry bulk density, loss-on-ignition organic matter, loosely-bound P, iron-bound P, labile organic P, aluminum-bound P, and total Al.

Spatial variations. Sediment cores were collected along a grid in June and late August 2017 to examine changes in sediment characteristics. Sediment sections were analyzed for percent moisture content, wet and dry bulk density, loss-on-ignition organic matter content, loosely-bound P, iron-bound P, aluminum-bound P, and total sediment aluminum. Sediment section thicknesses were different between the dates due to an error. The upper 10-cm sediment section was collected in June while the upper 5-cm was sectioned for analysis in late August. Because iron-bound P concentrations are highest in the upper 5-cm section and decline to lower constant concentrations below the 5-cm depth (James 2014 and see Figure 19 in this report), the

concentration in June was adjusted for dilution effects caused by combining the entire 10-cm into a composite sample for direct comparison with samples for iron-bound P collected in late August.

Laboratory-derived diffusive phosphorus flux from sediments under anaerobic conditions.

Anaerobic diffusive P fluxes were measured from intact sediment cores collected at stations shown in Figure 1. One sediment core was collected at each station in June and late August to monitor alum treatment effectiveness after application. Replicate (3 each) intact sediment cores were also collected at WQ 2 for determination of anaerobic diffusive P flux. The sediment incubation systems were placed in a darkened environmental chamber and incubated at 20 C for up to 6 days. The incubation temperature was set to a standard temperature for all stations for comparative purposes. The oxidation-reduction environment in each system was controlled by gently bubbling nitrogen through an air stone placed just above the sediment surface to maintain anaerobic conditions.

Water samples for soluble reactive P (SRP) were collected from the center of each system using an acid-washed syringe and filtered through a 0.45 μm membrane syringe filter (Nalge). The water volume removed from each system during sampling was replaced by addition of filtered lake water preadjusted to the proper oxidation-reduction condition. These volumes were accurately measured for determination of dilution effects. Rates of P release from the sediment ($\text{mg}/\text{m}^2 \text{ d}$) were calculated as the linear change in mass in the overlying water divided by time (days) and the area (m^2) of the incubation core liner. Regression analysis was used to estimate rates over the linear portion of the data.

Analytical methods. A known volume of sediment was dried at 105 °C for determination of moisture content, wet and dry bulk density, and burned at 550 °C for determination of loss-on-ignition organic matter content (Avnimelech et al. 2001, Håkanson and Jansson 2002). Phosphorus fractionation was conducted according to Hieltjes and Lijklema (1980), Psenner and Puckso (1988), and Nürnberg (1988) for the determination of ammonium-chloride-extractable P (loosely-bound P), bicarbonate-dithionite-extractable P (i.e., iron-bound P), and sodium hydroxide-extractable P (i.e., aluminum-bound P). Additional sediment was dried to a constant

weight, ground, and digested for analysis of total Al.

The loosely-bound and iron-bound P fractions are readily mobilized at the sediment-water interface as a result of anaerobic conditions that lead to desorption of P from sediment and diffusion into the overlying water column (Mortimer 1971, Boström et al. 1982, Boström 1984, Nürnberg 1988). The sum of the loosely-bound and iron-bound P fraction represents redox-sensitive P (i.e., the P fraction that is active in P release under anaerobic and reducing conditions) and will be referred to as *mobile P*. Aluminum-bound P reflects P bound to the Al floc after aluminum sulfate application and its chemical transformation to aluminum hydroxide (Al(OH)₃).

Summary of Results

Hydrology and phosphorus loading

On an annual basis, precipitation in 2017 was slightly higher at ~39 inches compared to the ~ 33-inch average since 1980 (Fig. 2). Monthly precipitation exceeded the long-term average in May, June, August, and October 2017 (Fig. 3). Precipitation in May 2017 was ~ 2X greater than the long-term average. Monthly precipitation was less than the long-term average in July and September 2017.

Horse Creek summer flow was elevated in May and June 2017 in conjunction with above average precipitation and declined in July through September 2017 (Fig. 4). Smaller peaks in flow occurred during precipitation events in early to mid-August and late September to October 2017. Horse Creek mean summer (May-October) flow was 0.58 m³/s, which fell within ranges between 2009-2011 (James 2014; 2009 = 0.44 m³/s, 2010 = 0.50 m³/s, 2011 = 0.67 m³/s). Total P and SRP concentrations were elevated during storm inflows in May through early July and declined to lower concentrations during nominal flows between mid-July and August (Fig. 5). A second P concentration peak occurred in Late September that was associated with a Fall storm-related elevated flow in Horse Creek. Overall, concentration-flow relationships in 2017 were like those in 2009-2011 (Fig. 6). Flow-averaged summer total P and SRP in 2017 were 0.084 mg/L

and 0.034 mg/L, respectively, similar to averages reported in James (2014). The flow-averaged SRP concentration accounted for ~ 40% of the total P in 2017. Summer (May through October) total P and SRP loading from Horse Creek were 4.26 and 1.71 kg/d, respectively, similar to previous research in 2009-11.

Lake limnological response

Cedar Lake was stratified between mid-May and mid-August 2017 (Fig. 7). Complete water column mixing and turnover occurred in late August 2017. During the period of alum application, stratification temporarily weakened because of a cold front and cooler air temperatures in late June. Bottom water anoxia developed between late May and August; however, the vertical extent of anoxia above the sediment interface was less compared to 2010. This pattern may have been related to reduced algal productivity, resulting in less organic carbon deposition to fuel sediment dissolved oxygen demand. Anoxic conditions extended to 6 m between late July and mid-August 2017. By comparison, anoxia between 6 m and the lake bottom occurred over a much longer period in 2010, i.e., early June and mid-August.

After the alum treatment, total P and SRP concentrations declined substantially in the bottom waters (i.e., ~ 7.5 m depth) during the entire summer stratified period and into fall turnover of 2017 despite hypolimnetic anoxia (Fig. 8). In particular, bottom water SRP ranged between only < 0.005 mg/L and 0.068 mg/L between July and August 2017 compared to much higher P concentrations during the same period in 2010 (0.039 mg/L to 1.092 mg/L). Surface total P concentrations declined to 0.027 mg/L in July 2017 after the alum treatment and gradually increased to a peak 0.081 mg/L in early October 2017 (Fig. 8). In contrast, surface total P concentrations increased from ~ 0.042 mg/L in early July to 0.111 mg/L in early October 2010.

Surface chlorophyll exhibited a similar seasonal response to the 2017 alum treatment (Fig. 9). The concentration declined to ~ 13 µg/L in July 2017 immediately after the alum treatment and remained relatively low until early August. Concentrations then increased rapidly to a peak ~ 43 µg/L in conjunction with the onset of Fall turnover in August through early September 2017. Importantly, however, chlorophyll declined from this peak and concentrations were modest,

ranging between 24 and 29 $\mu\text{g/L}$, between mid-September and October 2017.

The typical seasonal chlorophyll pattern in years prior to alum treatment was a substantial increase concentration during Fall turnover due to entrainment of hypolimnetic SRP and uptake by cyanobacteria (James et al. 2015). For instance, in 2010 chlorophyll increased from $\sim 22 \mu\text{g/L}$ in mid-July to a maximum $\sim 110 \mu\text{g/L}$ in early October (Fig. 9). Unlike Fall patterns in 2017, chlorophyll concentrations remained high and maximal for extended periods (i.e., September through early November) during Fall turnover as in 2010. Thus, reduced hypolimnetic SRP availability as a result of alum treatment in 2017 led to much lower chlorophyll concentrations during the Fall turnover period.

Overall, Secchi transparency improved in conjunction with alum treatment in 2017 (Fig. 10). Prior to alum treatment, as in 2010, Secchi transparency was often unusually high in June, exceeding 2 to 3 m (James 2014, 2015). Transparency declined to a minimum (< 1.0 m) during periods of extended cyanobacteria blooms driven by Fall turnover and hypolimnetic SRP entrainment (Fig. 10, 2010). In 2017, Secchi transparency increased to nearly 3 m immediately after the alum treatment (July through early August). It declined rapidly and substantially in mid-August, coincident with the modest algal bloom, but then increased linearly to ~ 2 m in October 2017. In general, water clarity was much improved during the Fall turnover period of 2017 compared to much lower transparencies in 2010 (Fig. 10). Secchi transparency exhibited a significant inverse pattern to that of chlorophyll, indicating that light extinction was due to algae versus inorganic turbidity (Fig. 11).

A comparison of mean summer (July-early October) limnological response variables before (i.e., 2010) and after (i.e., 2017) alum treatment is shown in Figure 12. Compared to the summer of 2010, alum treatment in 2017 resulted in a substantial reduction in bottom concentrations of total P and SRP. Bottom total P and SRP declined by 85% and 92%, respectively, in conjunction with the 2017 alum application. Mean summer surface total P and chlorophyll declined by 31% and 47%, respectively, while Secchi transparency improved by 46% due to the 2017 alum treatment.

Seasonal increases in Cedar Lake P mass were modest in 2017 as a result of alum treatment

compared to 2010 (Fig. 13). For instance, peak lake P mass was only 1,924 kg in 2017 compared to a maximum of > 4,000 kg in 2010. As indicated in James (2014, 2015), summer P mass increases were due almost entirely to internal P loading from anoxic sediment prior to alum treatment. Net internal P loading was substantial in 2010 at 3,723 kg (Table 1). In contrast, net internal P loading declined substantially to 1,150 kg in 2017 (Table 1). Thus, the 2017 net internal P loading rate represented a 69% reduction over the rate estimated for 2010. When normalized with respect to the time period used in the estimation of net internal P loading (kg/d), the rate was much lower in 2017 at 14 kg/d versus 2010, representing a 64% improvement over the 2010 rate of 38 kg/d (Table 1).

The pattern of seasonal P mass increase in the epilimnion versus the hypolimnion also changed in conjunction with the 2017 alum treatment (Fig. 14). For instance, the anoxic hypolimnion accounted for most of the of the seasonal P mass increase in 2010 (Fig. 14, please note scale differences). By comparison, hypolimnetic P mass accumulation was minor in 2017 because of the alum treatment, indicating suppression of net internal P loading (Fig. 14). Remarkably, P mass increase was actually greater in the epilimnion versus the hypolimnion in 2017 (Table 2). This pattern was unusual in that there was no apparent link between the modest cyanobacterial bloom and internal P loading. Rather, chlorophyll exhibited a modest bloom in 2017 despite apparently low hypolimnetic P. This pattern suggested that cyanobacteria may have directly accessed sediment P while dormant on the lake bottom as resting cells (i.e., akinetes) and then inoculated the epilimnion in August through early September (see Summary and Recommendations section).

Changes in sediment chemistry and anaerobic diffusive phosphorus flux

The goal of the 2017 treatment was application of an Al concentration of ~ 20 g/m² between the 20 and 25-ft contour and an Al concentration of ~ 26 g/m² to depths > 25 ft. The mean surface Al concentration for depths > 20 ft was 27.2 g/m² (± 0.8 SE), close to the overall target (Fig. 15). Spatially, Al concentration fell below the target some stations located in the north region of the lake (stations, 0, 1, 2, 3, 7, and 8, Fig. 16). Concentrations were anonymously high at station 5 and 6. However, the Al concentration fell within the 20-26 g/m² range for all other stations (Fig.

16).

Anaerobic diffusive P fluxes and sediment mobile P (i.e., the sum of loosely-bound P and iron-bound P), adjusted to the upper 5-cm surface layer, and were higher in June 2017 compared to rates and concentrations determined in June 2012 (Figs. 17 and 18) and reported in James (2014), suggesting that the potential for high internal P loading had perhaps increased since previous research conducted between 2009 and 2012. Mobile P concentrations also increased in the upper 2 cm sediment layer at station 2 in June 2017 compared to June 2012 (Fig. 19).

Laboratory-derived anaerobic diffusive P fluxes declined substantially at most stations in August 2017 after alum treatment (Fig. 20). Diffusive P flux reduction was minimal at stations 1 and 2, located along the north edge of the treatment area and stations 21, 22, and 23, located along the south edge of the treatment area. However, diffusive P fluxes at most other stations in August represented between ~20% to > 80% decline over fluxes measured in June.

When all stations were considered, anaerobic diffusive P flux decreased by a mean 37% from June (mean rate = $15.01 \text{ mg/m}^2 \text{ d} \pm 0.85 \text{ SE}$) to August (mean rate = $9.53 \text{ mg/m}^2 \text{ d} \pm 0.78 \text{ SE}$, Fig. 21). Although the percent decline was important, the mean August anaerobic diffusive P flux was still relatively high at $9.53 \text{ mg/m}^2 \text{ d}$. However, hypolimnetic anoxia was much less in 2017 at an average summer depth of ~ 7 m and sediment anoxic area of $2,043,101 \text{ m}^2$ for ~ 83 days. The anoxic factor was 40 d/summer which would represent a gross internal P flux of 1,676 kg/summer (i.e., $9.53 \text{ mg/m}^2 \text{ d} \times 40 \text{ d/summer} \times 4.36 \text{ km}^2 \times 0.000001 \text{ kg/mg}$), close to the net internal P loading rate of 1,150 kg estimated via P mass balance (Table 1). Laboratory incubations represent a gross flux of P out of the sediment while P mass balance reflects a net flux of P diffusion out of sediment minus deposition back to the sediment. Typically, P fluxes determined from laboratory incubations are greater than those estimated from P mass balance (Nürnberg 2009).

Most stations, particularly those within the 25-ft contour, exhibited a decline in mobile P (i.e., the sum of loosely-bound and iron-bound P) in the upper 5-cm sediment layer in August 2017 after the alum treatment (Fig. 22), suggesting some binding and inactivation of sediment P

fractions correlated with internal P loading. The percent decrease in mobile P ranged between negligible to 89% inactivation and the mean percent decrease over all stations was 37% between Jun and August 2017 (Fig. 21). The mean concentration difference between June and August 2017 was 0.18 mg/g mobile P.

Changes in the aluminum-bound P fraction in the upper 5-cm sediment layer represented binding of mobile P from the water column during initial application and additional binding from the sediment mobile P pool after formation of the Al floc layer on top of the sediment. Nearly all stations exhibited an increase in aluminum-bound P after the alum treatment, suggesting some binding and inactivation of mobile P (Fig. 23). Overall, mean aluminum-bound P increased in the upper 5-cm sediment layer by ~65% (Fig. 21). However, the mean increase in aluminum-bound P between June and August 2017 was less at 0.063 mg/g than the mean loss of mobile P at 0.18 mg/g. The discrepancy is likely due to known interferences in the fractionation sequence that result in inefficient recovery of aluminum-bound P (Huser and Pilgrim 2014).

Vertically in the sediment column at station 2 concentrations of mobile P were greatest in the upper 5-cm layer and declined to a constant lower concentration below 8 cm in June 2017 before alum treatment (Fig. 24). After the alum treatment, concentrations declined within the upper 5-cm sediment layer, suggesting some binding of mobile P by the Al floc. The mobile P concentration decline in that layer was ~ 0.282 mg/g or ~ 48% reduction. This pattern coincided with a substantial reduction in the mean anaerobic diffusive P flux at station 2 (Fig. 25). Before the alum treatment, the diffusive P flux at station 2 was 17.7 mg/m² d. The flux declined to 7.6 mg/m² d at this station in August after the alum treatment, representing a 57% reduction.

Aluminum-bound P concentrations increased in the upper 5-cm layer in August after the alum treatment, suggesting binding of P by the Al floc (Fig. 24). Similar to the spatial sediment P analysis, the net aluminum-bound P concentration increase of 0.121 mg/g was less than the net decrease in mobile P (0.282 mg/g).

Summary and recommendations

The alum treatment appeared to meet target Al concentration goals and was successful in substantially reducing SRP concentration increases in the hypolimnion and net internal P loading estimated from P mass balance in 2017. Mean summer (July-October) chlorophyll declined from 47 $\mu\text{g/L}$ in 2010 to only 25 $\mu\text{g/L}$ in 2017, representing a 47% decrease in concentration (Table 3). Despite lower net internal P loading and hypolimnetic SRP, a modest algal bloom developed in conjunction with turnover in late August through early September 2017. Although peak chlorophyll reached 43 $\mu\text{g/L}$ during this bloom, concentrations were much lower compared to pretreatment periods of Fall turnover (for instance, 2010) when peak concentrations exceeded 100 $\mu\text{g/L}$ (Table 3). In addition, the 2017 Fall bloom was short-lived as concentrations declined in late September through October 2017. Thus, the 2017 alum treatment was effective in reducing the severity and magnitude of the Fall algal bloom that typically developed prior to alum treatment.

The development of a modest Fall algal bloom was unusual considering the very low hypolimnetic SRP concentrations and lack of watershed P loading in July and August 2017. Although laboratory-derived anaerobic diffusive P fluxes were reduced by 37% after the alum treatment, the mean flux was nevertheless high, suggesting internal P loading could have subsidized the bloom in 2017. Sediment mobile P concentrations also declined by 37% in conjunction with the alum treatment. However, post-treatment mobile P concentrations were not completely controlled by the Al floc and could have remained a source for algal uptake. Algal resting cells or akinetes residing in the sediment prior to the alum treatment could have stored surplus P (i.e., luxury P uptake) derived from the sediment and later inoculated the water column during the onset of turnover, resulting in initial modest growth and bloom formation in late August. However, the lack of any additional available SRP in the water column as a result of the alum application hindered further growth, resulting in much lower peak chlorophyll and a short-lived bloom relative to other years.

A similar bloom phenomenon occurred in Half Moon Lake immediately after a 150 g/m^2 alum treatment in June 2011 (James 2012, 2017). Although sediment internal P loading was 100%

inactivated, the cyanobacteria *Cylindrospermopsis* sp. inoculated the water column and chlorophyll concentrations increased to ~ 40 µg/L by September 2011. This unusual pattern was attributable to a couple of factors that resulted in its unexpected success. This species overwinters as a spore or cyst in the sediment and probably assimilated luxury P (i.e., P stored in cells as polyphosphates well in excess of growth requirements) from the sediment before the alum treatment occurred. These reserves were used in bloom development after excystment, providing the population a competitive advantage over other species that did not scavenge P before the alum treatment. *Cylindrospermopsis* did not bloom in 2012 or 2013 and chlorophyll concentrations were much lower, suggesting that spores were P limited after the alum treatment. Similar P luxury uptake by cyanobacterial akinetes residing in sediment could have occurred in Cedar Lake prior to the alum treatment.

Overall lake water quality improved substantially considering the low alum dosage applied to Cedar Lake in 2017. Using 2010 as a benchmark for pretreatment trends, alum application resulted in improvements in both mean summer (July-early October) and Fall maxima in limnological response variables (Table 3). Mean summer bottom total P and SRP declined by > 85% in 2017 versus 2010, reflecting substantially reduced net internal P loading in 2017 (> 60% reduction, Table 3). Mean summer and Fall peak chlorophyll concentration also declined in 2017 by 47% and 61%, respectively, compared to 2010, resulting in improved mean summer and Fall peak Secchi transparency (Table 3). In particular, mean summer chlorophyll was only 25 µg/L in 2017 versus 48 µg/L in 2010. Fall peak chlorophyll declined by 61% from 110 µg/L in 2010 to 43 µg/L in 2017 (Table 3).

Currently, lower dose alum treatments are scheduled to occur every third year until 2029 (Table 4). This treatment schedule was developed to 1) spread costs for alum out over a longer time period and into smaller cost increments and 2) increase overall Al binding efficiency and binding capacity by exposing lower Al doses to sediment and hypolimnetic P. Monitoring and adaptive management approaches are being used to assess water quality and sediment response in order to adjust application timing and Al dosage if necessary to meet goals and expectations.

While it is difficult to predict lake water quality response in 2018, there is concern that net

internal P loading will increase, resulting in higher mean summer and Fall peak chlorophyll with increased risk to human health via potential cyanotoxicity before the next scheduled alum treatment in 2020. Although the current Al floc should continue to bind sediment mobile P, binding efficiency is anticipated to decline by 2018 as demonstrated by other research (de Vicente et al. 2008), which could result in higher net internal P loading if anaerobic diffusive P flux from sediment exceeds P binding by the Al floc. While this potential outcome was expected at the outset of planning and management of Cedar Lake, moving the next partial Al dose application from 2020 to 2018 or 2019 would mitigate this potential human health risk in the short-term by maintaining improved water quality conditions.

References

APHA (American Public Health Association). 2011. *Standard Methods for the Examination of Water and Wastewater*. 22th ed. American Public Health Association, American Water Works Association, Water Environment Federation.

Avnimelech Y, Ritvo G, Meijer LE, Kochba M. 2001. Water content, organic carbon and dry bulk density in flooded sediments. *Aquacult Eng* 25:25-33.

de Vicente I, Huang P, Andersen FØ, Jensen HS. 2008. Phosphate adsorption by fresh and aged aluminum hydroxide. Consequences for lake restoration. *Environ Sci Technol* 42:6650-6655.

Håkanson L, Jansson M. 2002. *Principles of lake sedimentology*. The Blackburn Press, Caldwell, NJ USA.

Hjieltjes AH, Lijklema L. 1980. Fractionation of inorganic phosphorus in calcareous sediments. *J Environ Qual* 8: 130-132.

James WF. 2012. *Limnological and aquatic macrophyte biomass characteristics in Half Moon Lake, Eau Claire, Wisconsin, 2012: Interim letter report*. University of Wisconsin – Stout, Sustainability Sciences Institute – Discovery Center, Menomonie, WI.

James WF. 2014. *Phosphorus budget and management strategies for Cedar Lake, WI*. University of Wisconsin – Stout, Sustainability Sciences Institute – Discovery Center, Menomonie, WI.

James WF. 2017. Phosphorus binding dynamics in the aluminum floc layer of Half Moon Lake, Wisconsin. *Lake Reserv Manage* 33:130-142.

James WF, PW Sorge, PJ Garrison. 2015. Managing internal phosphorus loading in a weakly stratified eutrophic lake. *Lake Reserv Manage* 31:292-305.

Mortimer CH. 1971. Chemical exchanges between sediments and water in the Great Lakes – Speculations on probable regulatory mechanisms. *Limnol Oceanogr* 16:387-404.

Nürnberg GK. 1988. Prediction of phosphorus release rates from total and reductant-soluble phosphorus in anoxic lake sediments. *Can J Fish Aquat Sci* 45:453-462.

Nürnberg GK. 2009. Assessing internal phosphorus load – Problems to be solved. *Lake Reserv Manage* 25:419-432.

Psenner R, Puckso R. 1988. Phosphorus fractionation: Advantages and limits of the method for the study of sediment P origins and interactions. *Arch Hydrobiol Biel Erg Limnol* 30:43-59.

Table 1. Summer net internal phosphorus loading ($P_{\text{net int load}}$) estimates (bold font) for Cedar Lake in 2010 (pretreatment) and 2017 (post-treatment).								
Summer	Period (d)	$P_{\text{tributary}}$ (kg)	$P_{\text{discharge}}$ (kg)	$P_{\text{retention}}$ (kg)	$P_{\text{lake storage}}$ (kg)	(kg)	$P_{\text{net int load}}$ (kg/d)	(mg/m ² d)
2010	97	445	238	207	3,931	3,723	38	8.8
2017	83	349	212	137	1,287	1,150	14	3.2

Table 2. Summer phosphorus mass accumulation rate in the entire lake water column, the epilimnion (i.e., upper 4 m), and the hypolimnion (i.e. 5 to 8 m) in 2010 (pretreatment) and 2017 (post treatment).			
(kg/d)	2010	2017	
Lake	40	16	
Epilimnion	4	13	
Hypolimnion	36	3	

Table 3. Summary of changes in lake water quality and sediment variables after the initial alum treatment in June 2017. Overall goals after completion of the treatment schedule (Table 4) are shown in the last column.

Variable		2010	2017	Percent improvement	Goal after internal P loading control	
Lake	Mean (Jul-Oct)	Mean surface TP (mg/L)	0.074	0.051	31% reduction	< 0.035
		Mean bottom TP (mg/L)	0.583	0.088	85% reduction	< 0.050
		Mean bottom SRP (mg/L)	0.467	0.038	92% reduction	< 0.050
		Mean chlorophyll (ug/L)	47.63	25.17	47% reduction	< 15
		Mean Secchi transparency (ft)	4.27	6.28	46% increase	12.1
	Early Fall peak (i.e. late August-early October)	Surface TP (mg/L)	0.130	0.081	38% reduction	NA
		Bottom TP (mg/L)	1.216	0.13	89% reduction	NA
		Bottom SRP (mg/L)	1.092	0.068	94% reduction	NA
		Chlorophyll (ug/L)	109.6	42.95	61% reduction	NA
		Secchi transparency (ft)	2.66	3.61	36% increase	NA
Sediment	Net internal P loading (kg/summer)	3,723	1,150	69% reduction	< 400	
	Net internal P loading (mg/m ² d)	8.8	3.2	64% reduction	< 1.5	
	Gross internal P loading from diffusive P flux and anoxic factor (kg/summer)	3,011	1,676	44% reduction	< 400	
	Sediment diffusive P flux (mg/m ² d)	15.01	9.53	37% reduction	< 1.5	
	Mobile P (mg/g)	0.457	0.276	37% reduction	< 0.100	

Table 4. Alum application schedule for Cedar Lake. Gray blocks represent treatment years.

Year	Al treatment
2017	
2018	
2019	
2020	
2021	
2022	
2023	
2024	
2025	
2026	
2027	
2028	
2029	
2030	

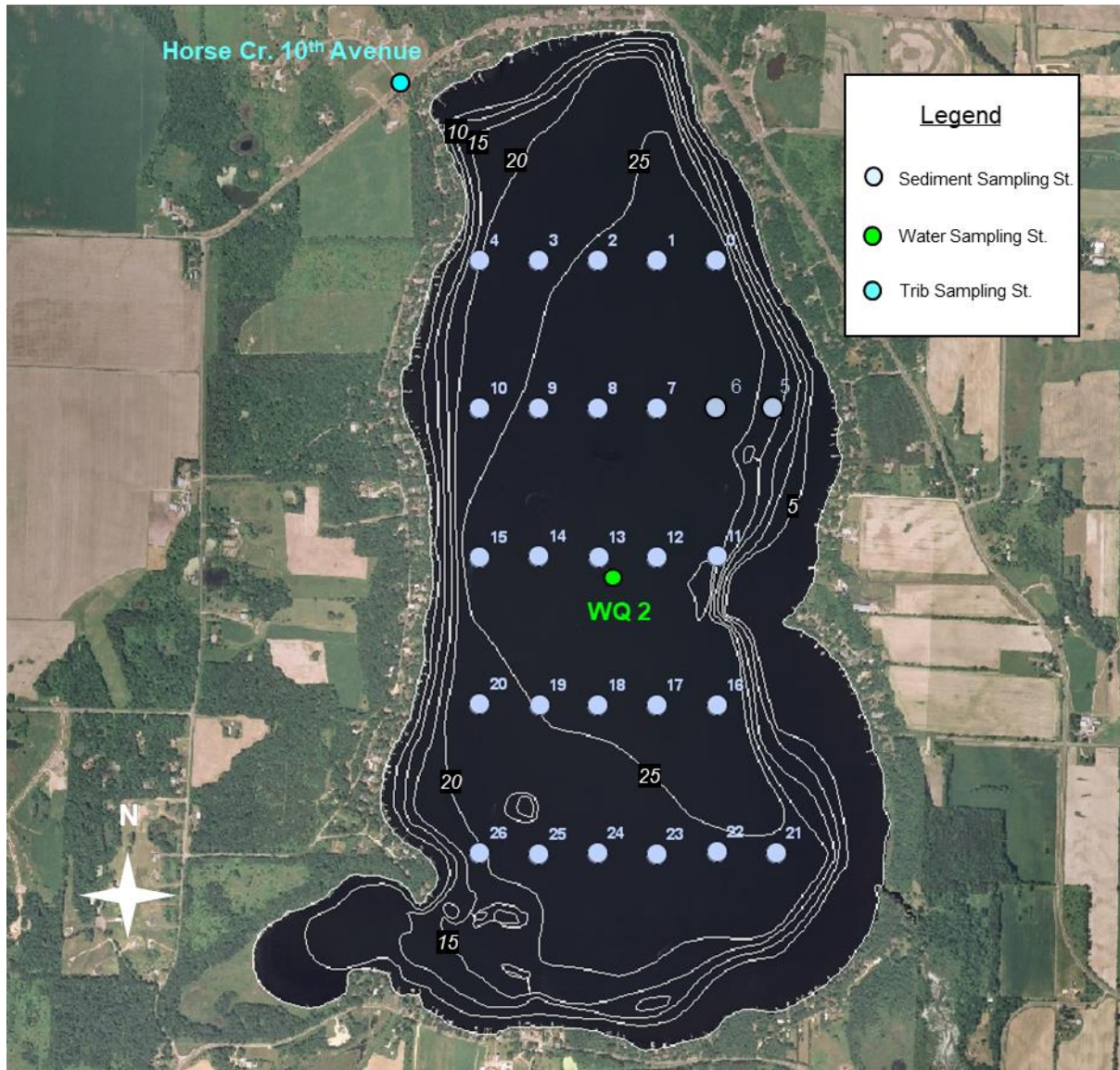


Figure 1. Sediment and water sampling stations.

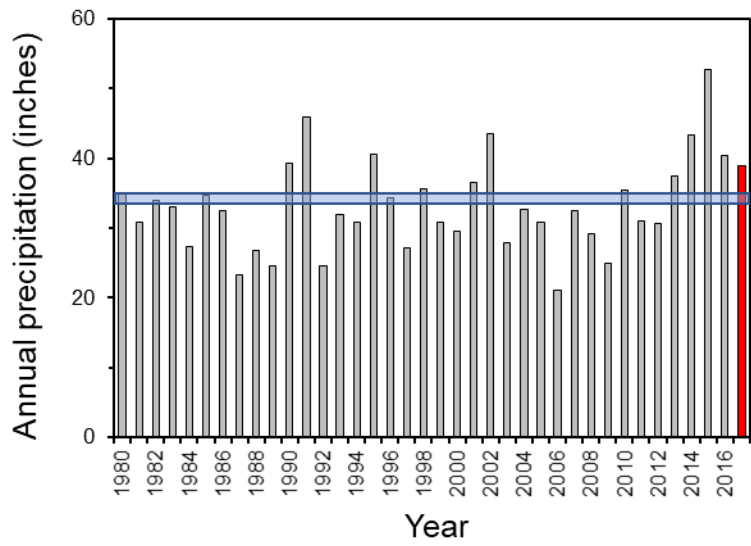


Figure 2. Variations in annual precipitation at Amery, WI. Blue horizontal line represents the average.

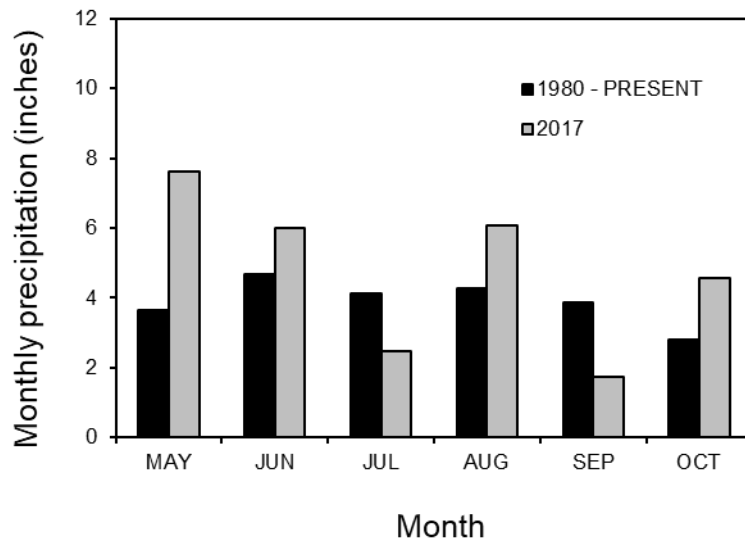


Figure 3. A comparison of average monthly precipitation.

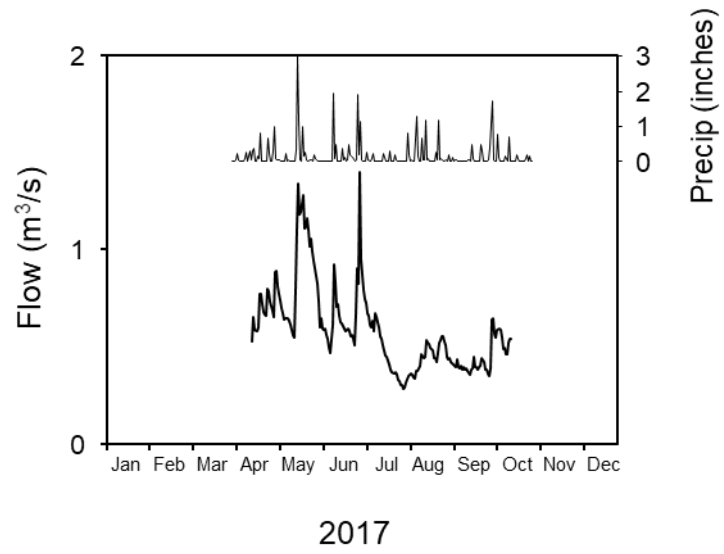


Figure 4. Seasonal variations in daily precipitation at Amery, WI, and flow for Horse Creek at 10th Ave.

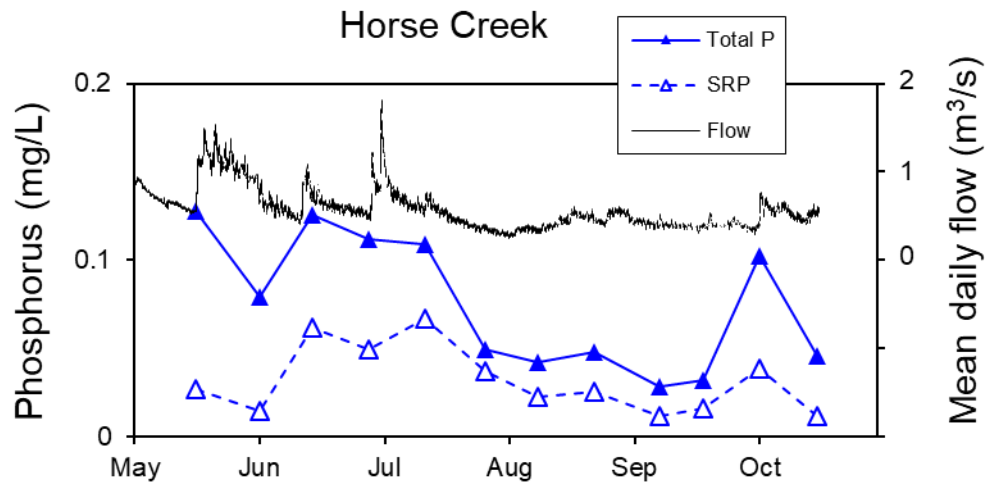


Figure 5. Seasonal variations in total phosphorus (P) and soluble reactive P (SRP) concentration at Horse Creek.

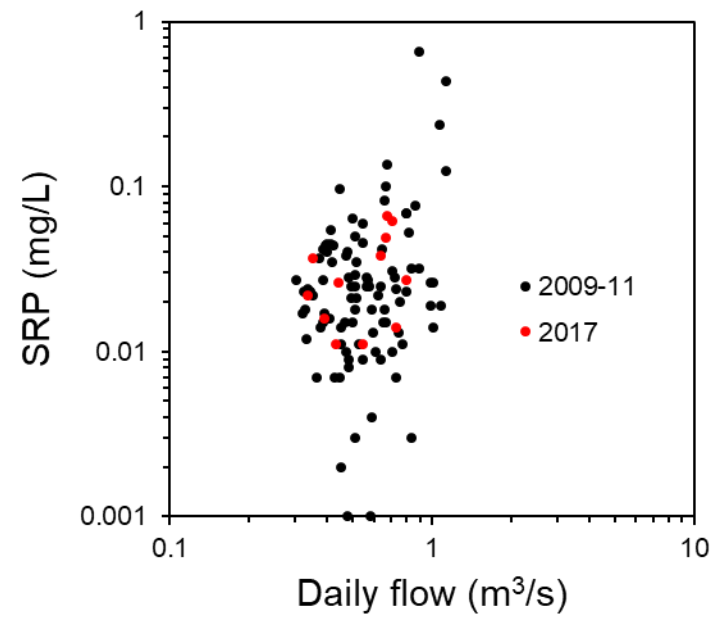
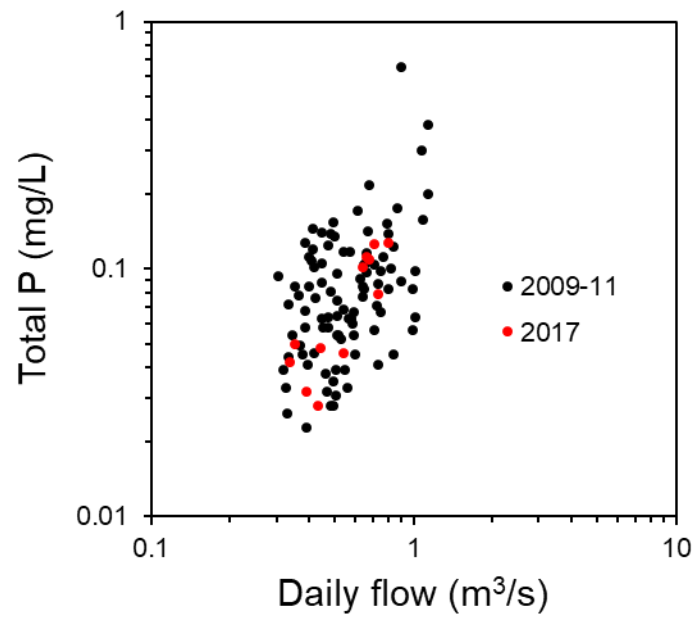


Figure 6. Phosphorus (P) concentration versus daily flow at Horse Creek.

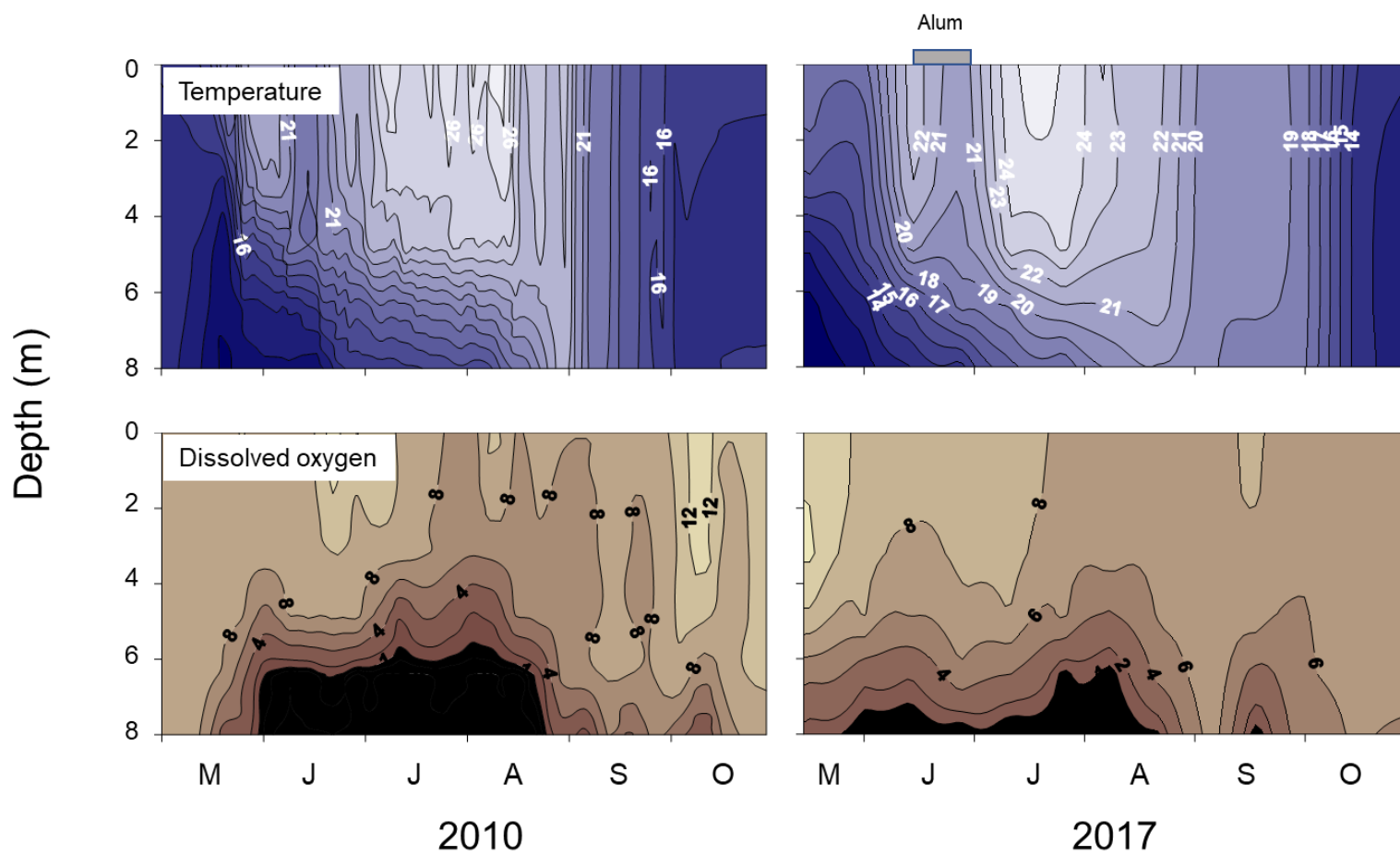


Figure 7. Seasonal and vertical variations in temperature (upper panel) and dissolved oxygen (lower panel) in 2010 (pre-treatment) and 2017 (the year of alum treatment).

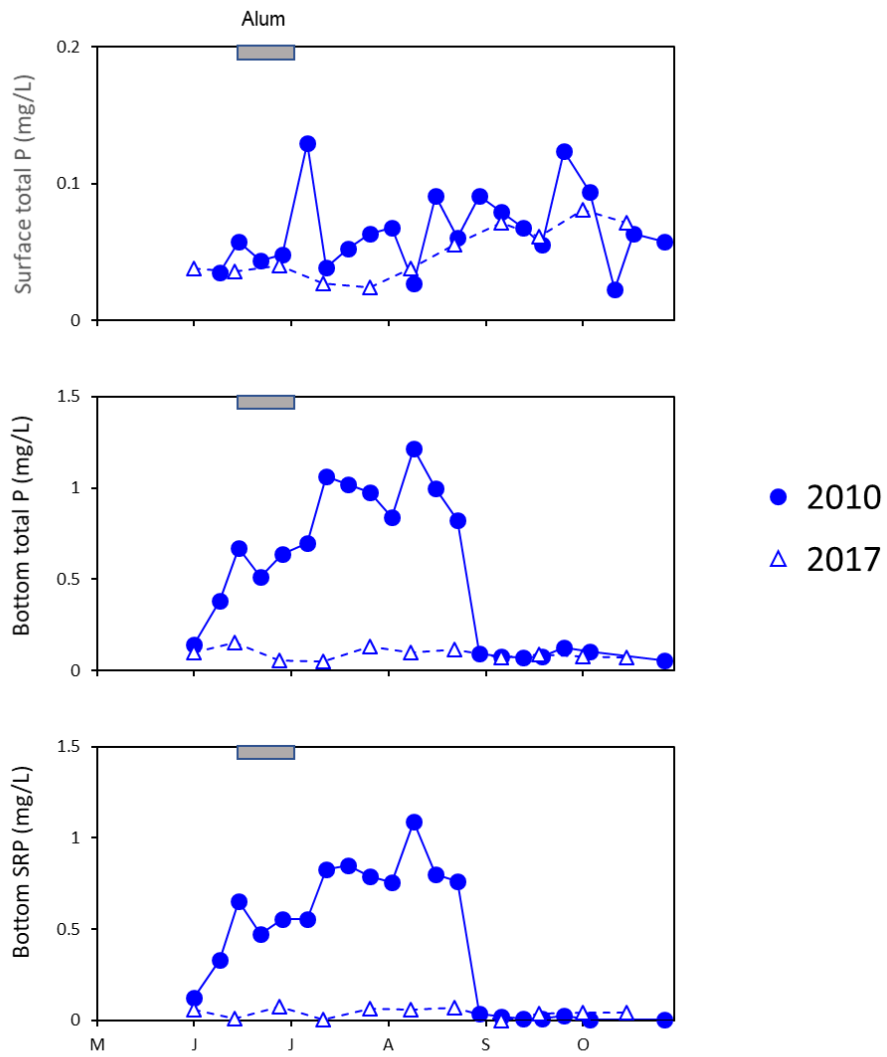


Figure 8. Seasonal variations in surface total phosphorus (P), bottom (i.e., ~ 0.25 m above the sediment-water interface) total P, and bottom soluble reactive P (SRP) during a pretreatment year (2010) and the year of alum treatment (2017).

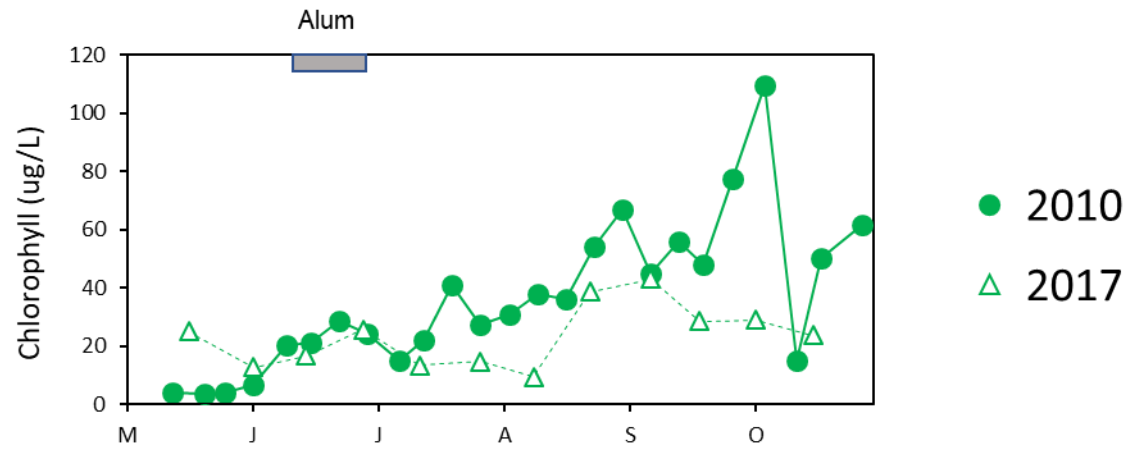


Figure 9. Seasonal variations in surface chlorophyll during a pretreatment year (2010) and the year of alum treatment (2017).

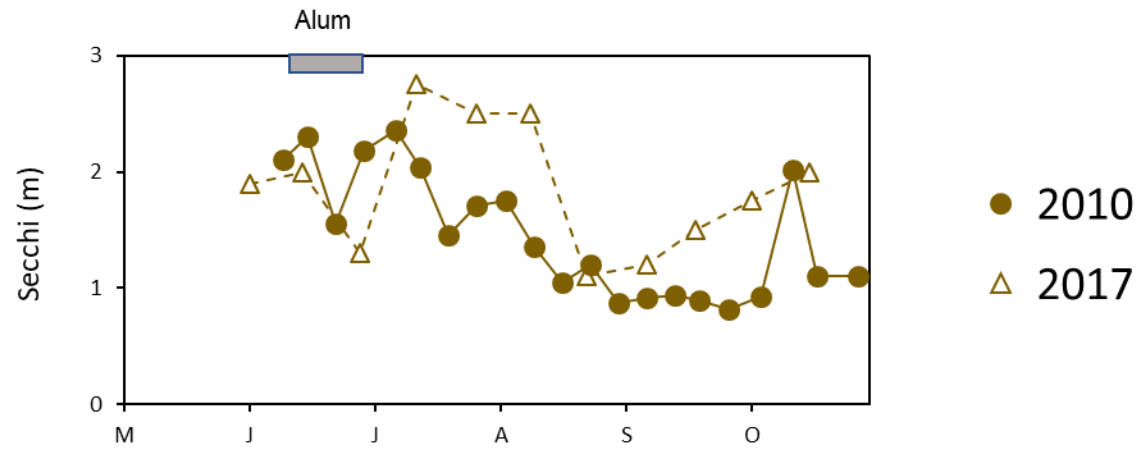
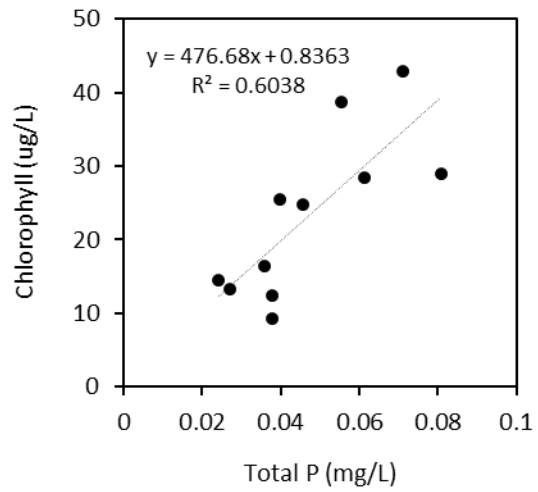
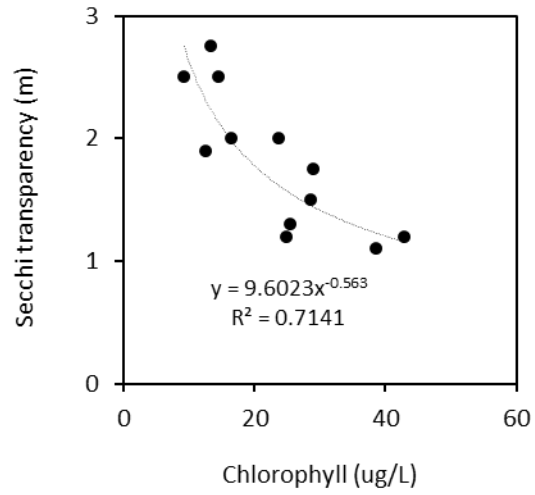
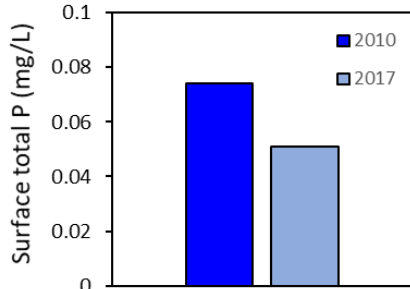


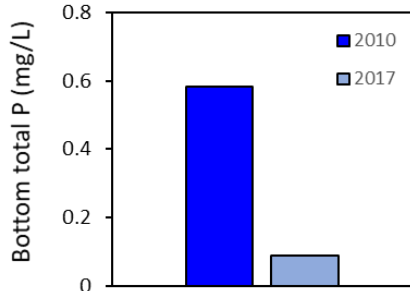
Figure 10. Seasonal variations in Secchi transparency during a pretreatment year (2010) and the year of alum treatment (2017).

Figure 11. Relationships between Secchi transparency and chlorophyll (upper panel) and total phosphorus (P) versus chlorophyll (lower panel) during the summer 2017.

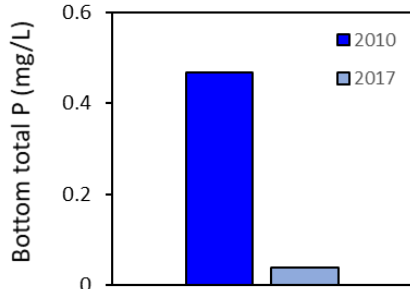




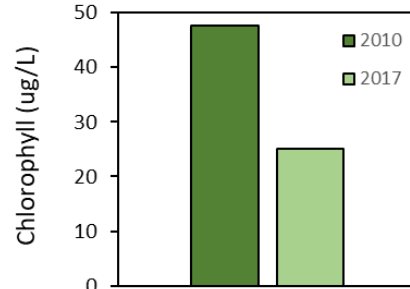
31% reduction



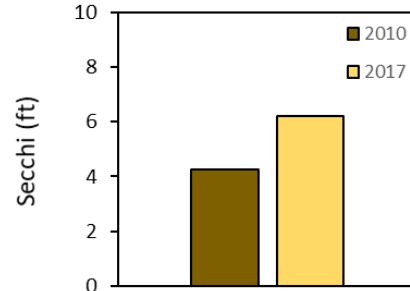
85% reduction



92% reduction



47% reduction



46% improvement

Figure 12. A comparison of mean summer (July-early October) summer concentrations of surface and bottom total phosphorus (P) and soluble reactive P (SRP), chlorophyll and Secchi transparency during a pretreatment year (2010) and the year of alum treatment (2017). Percent reduction or improvement between pre- and post-alum treatment are shown below each panel.

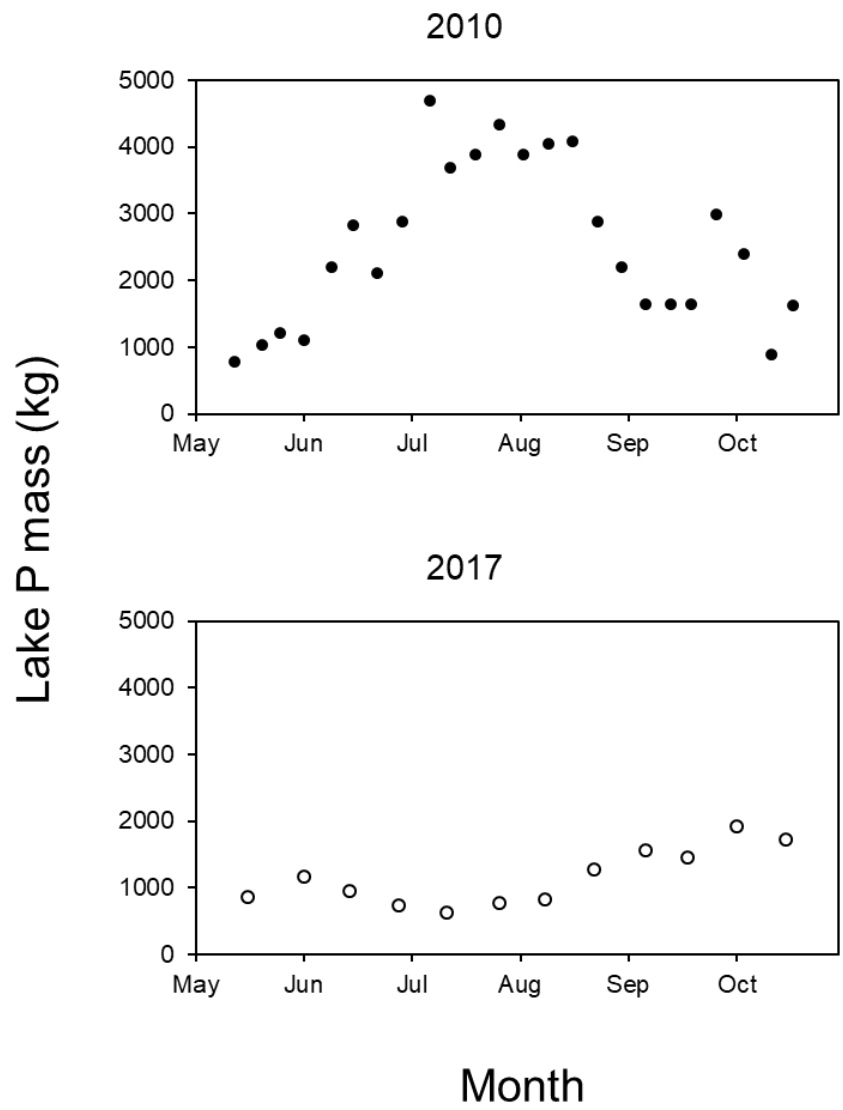


Figure 13. Seasonal variations in total phosphorus (P) mass during a pretreatment year (2010) and the year of alum treatment (2017).

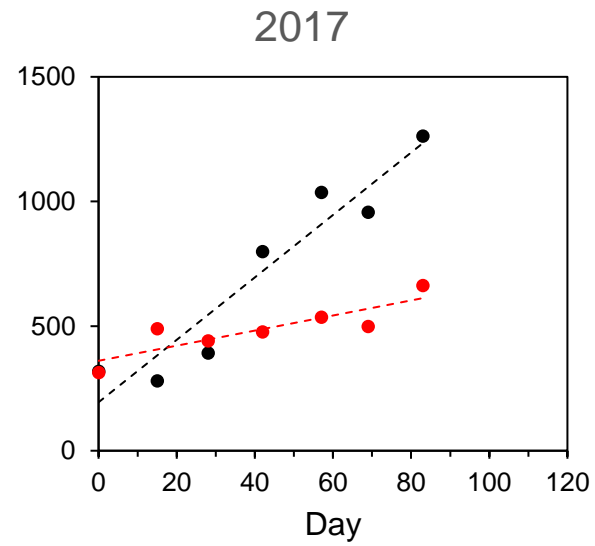
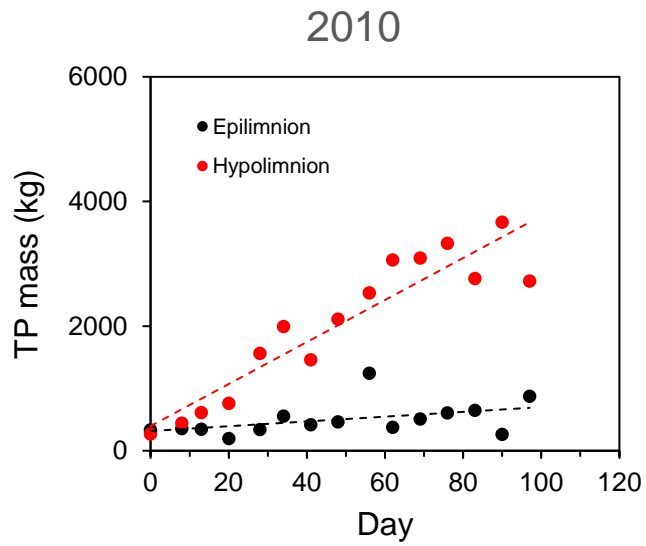


Figure 14. Seasonal variations in total phosphorus (P) mass in the epilimnion (i.e., 0-4 m) and hypolimnion (> 4 m) during a pretreatment year (2010) and the year of alum treatment (2017).

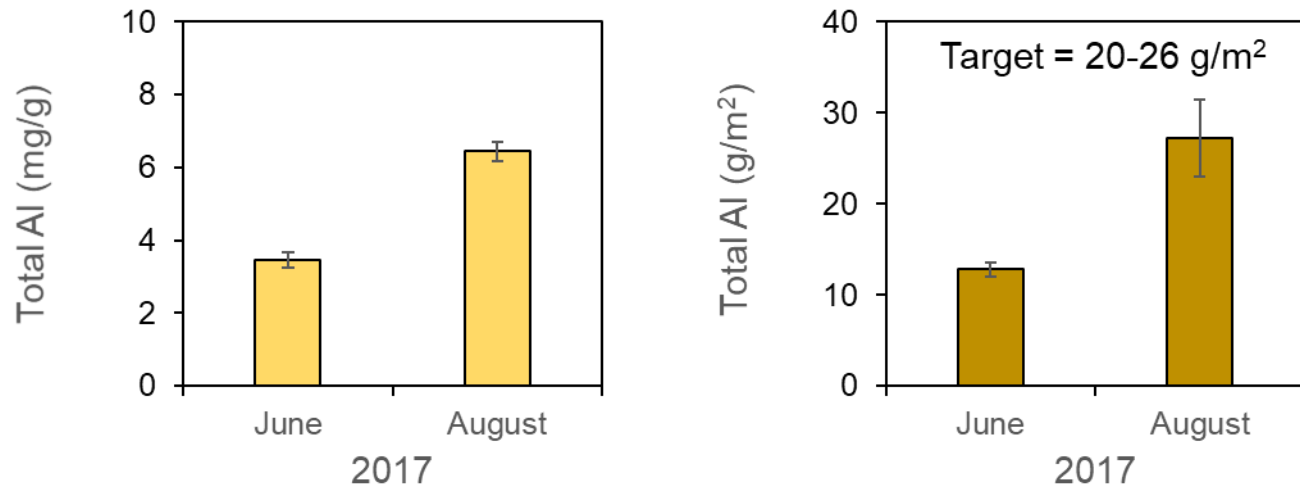


Figure 15. A comparison of mean sediment total aluminum (Al, n = 27, see Figure 1) before (June) and after (August) alum treatment in 2017. Horizontal lines represent ± 1 standard error.

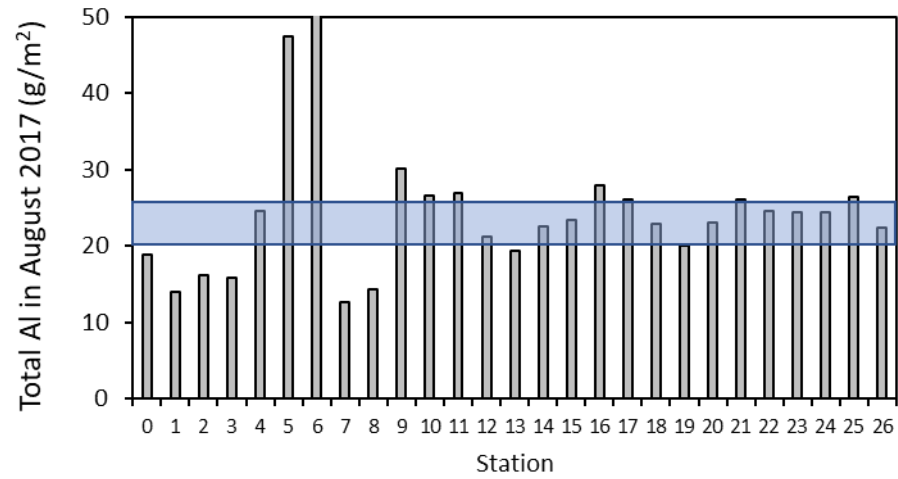


Figure 16. Sediment total aluminum (Al) concentrations in the upper 5-cm sediment layer for various stations in August after the 2017 alum treatment.

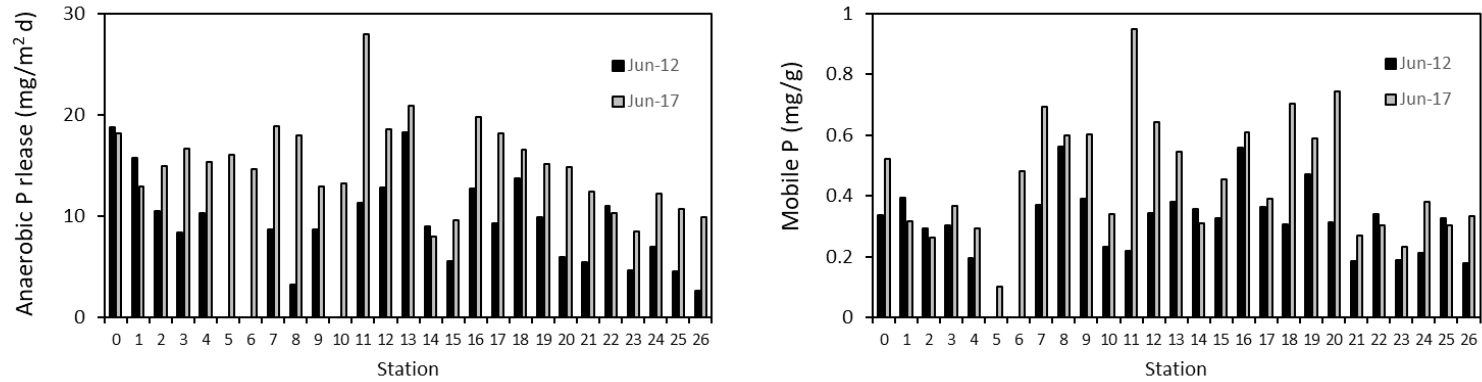


Figure 17. A comparison of rates of diffusive phosphorus (P) flux from sediment under anaerobic conditions (left) and sediment mobile (i.e., the sum of the loosely-bound P and iron-bound P sediment fractions) P concentrations adjusted for the upper 5-cm sediment layer for various stations (see Figure 1) in 2012 and 2017.

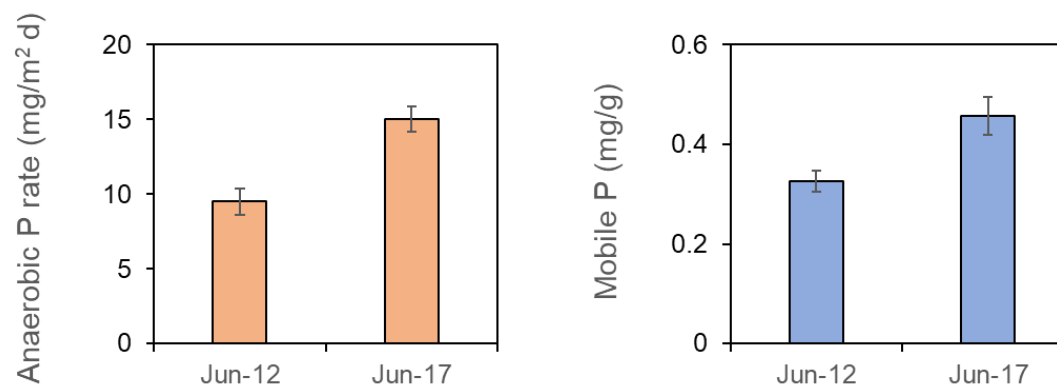


Figure 18. A comparison of mean ($n = 27$, see Figure 1) rates of diffusive phosphorus (P) flux from sediment under anaerobic conditions (left) and mean sediment mobile (i.e., the sum of the loosely-bound P and iron-bound P sediment fractions) P concentrations adjusted for the upper 5-cm sediment layer in 2012 and 2017. Horizontal lines represent ± 1 standard error.

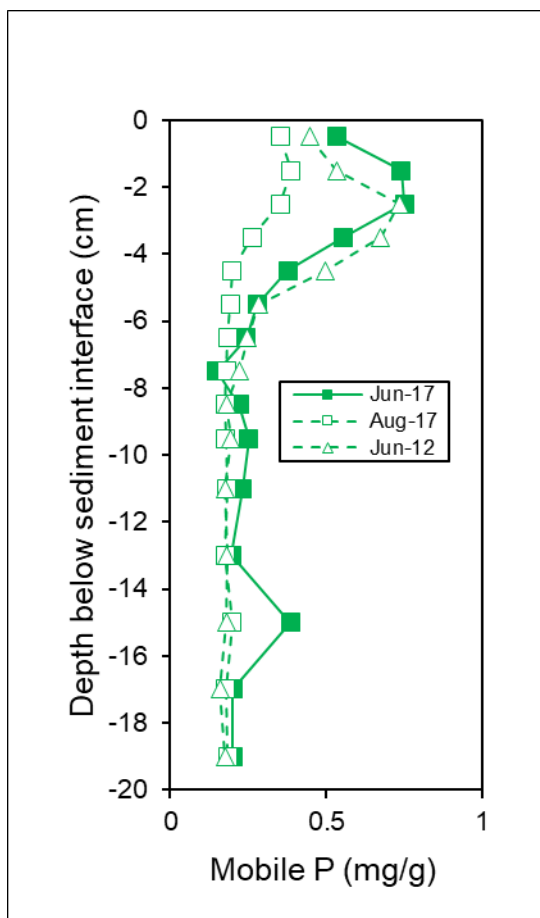


Figure 19. Vertical variations in sediment mobile (i.e., the sum of the loosely-bound P and iron-bound P sediment fractions) phosphorus (P) concentrations for a sediment core collected from station 2 (Figure 1) in June 2012, June 2017, and August 2017. The sediment profile in June of 2012 and 2017 represent pre-treatment conditions while August 2017 represents post-alum treatment conditions.

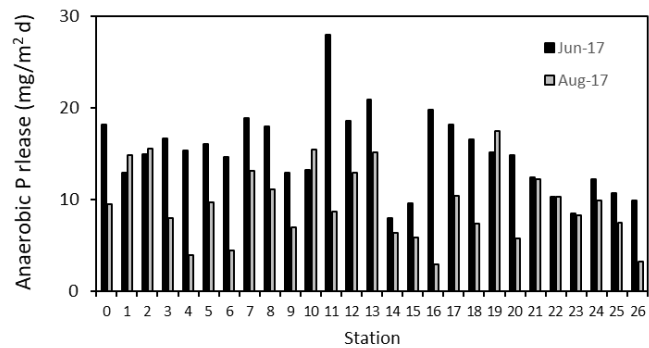
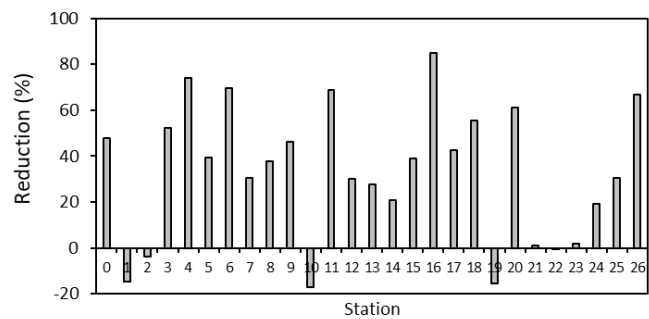
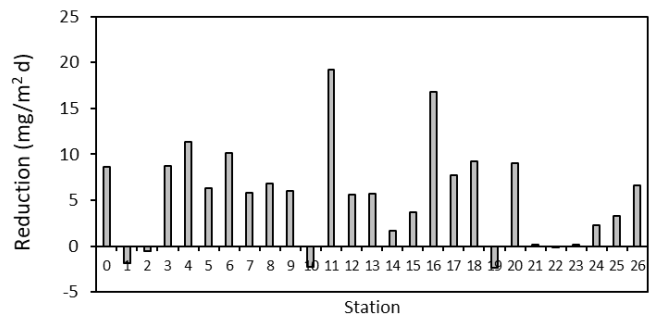


Figure 20. A comparison of anaerobic diffusive phosphorus (P) flux before (June 2017) and after (August 2017) alum application (upper panel), the change (reduction or increase) in flux as a result of the 2017 alum treatment (middle panel), and the percent reduction or increase in the anaerobic diffusive P flux (lower panel).



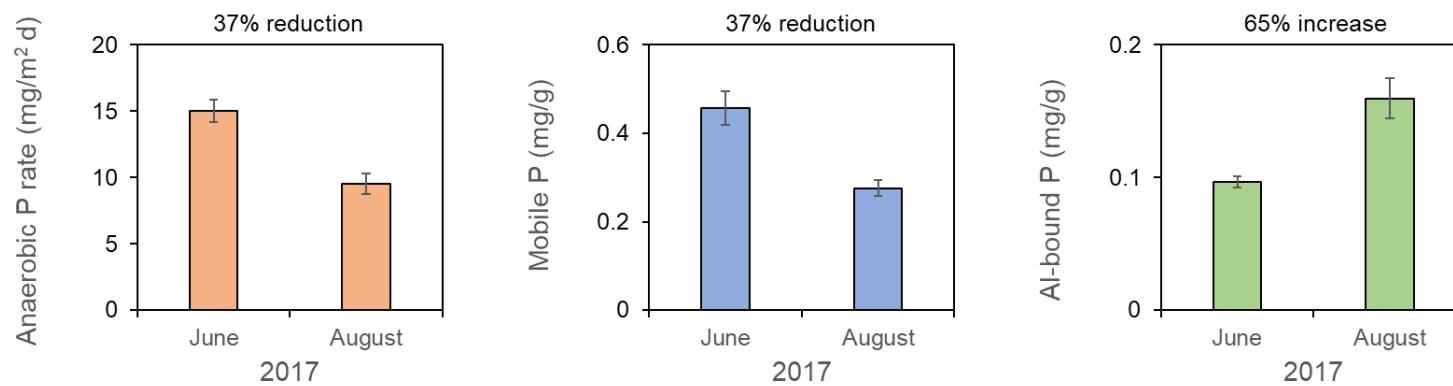


Figure 21. A comparison of mean anaerobic phosphorus (P) flux (left), mobile P (i.e., the sum of the loosely-bound and iron-bound P fractions, middle), and aluminum (Al)-bound P (right, $n = 27$, see Figure 1) before (June) and after (August) alum treatment in 2017. Horizontal lines represent ± 1 standard error.

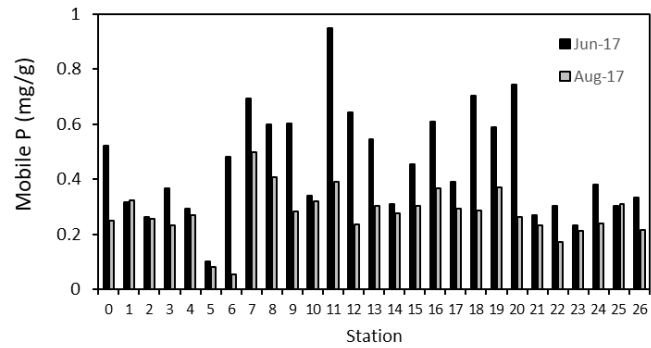
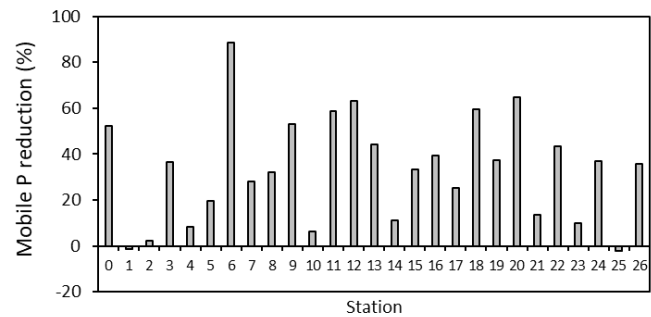
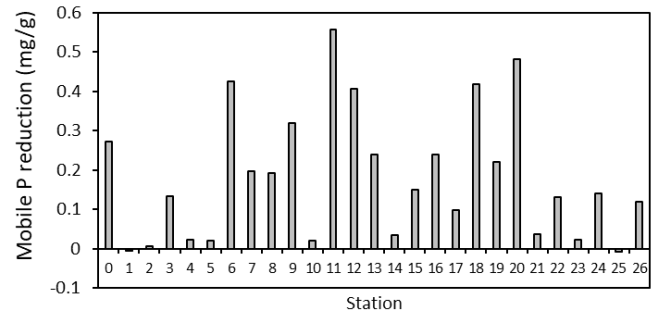


Figure 22. A comparison of mobile phosphorus (P) concentrations in the upper 5 cm sediment layer before (June 2017) and after (August 2017) alum application (upper panel), the change (reduction or increase) in concentration as a result of the 2017 alum treatment (middle panel), and the percent reduction or increase in the concentration (lower panel).



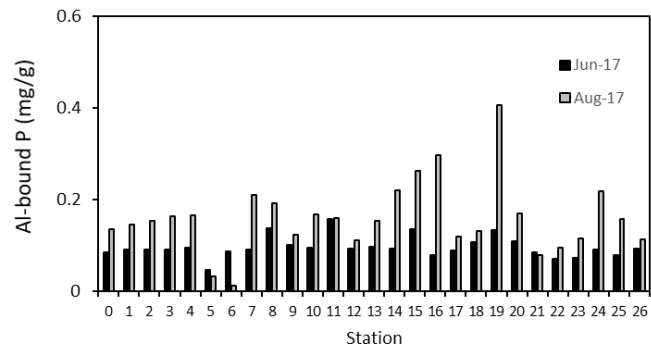
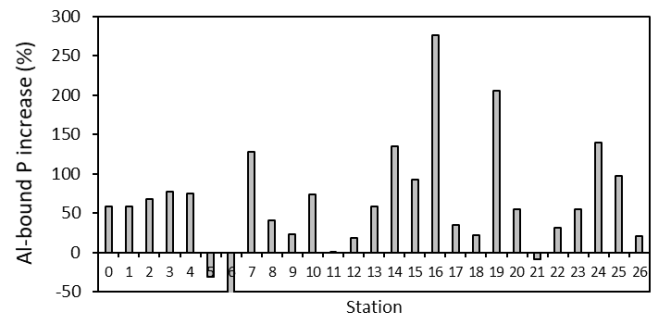
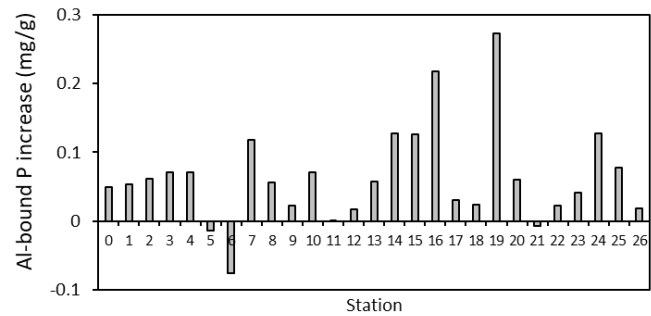


Figure 23. A comparison of aluminum (Al)-bound phosphorus (P) concentrations in the upper 5 cm sediment layer before (June 2017) and after (August 2017) alum application (upper panel), the change (reduction or increase) in concentration as a result of the 2017 alum treatment (middle panel), and the percent reduction or increase in the concentration (lower panel).



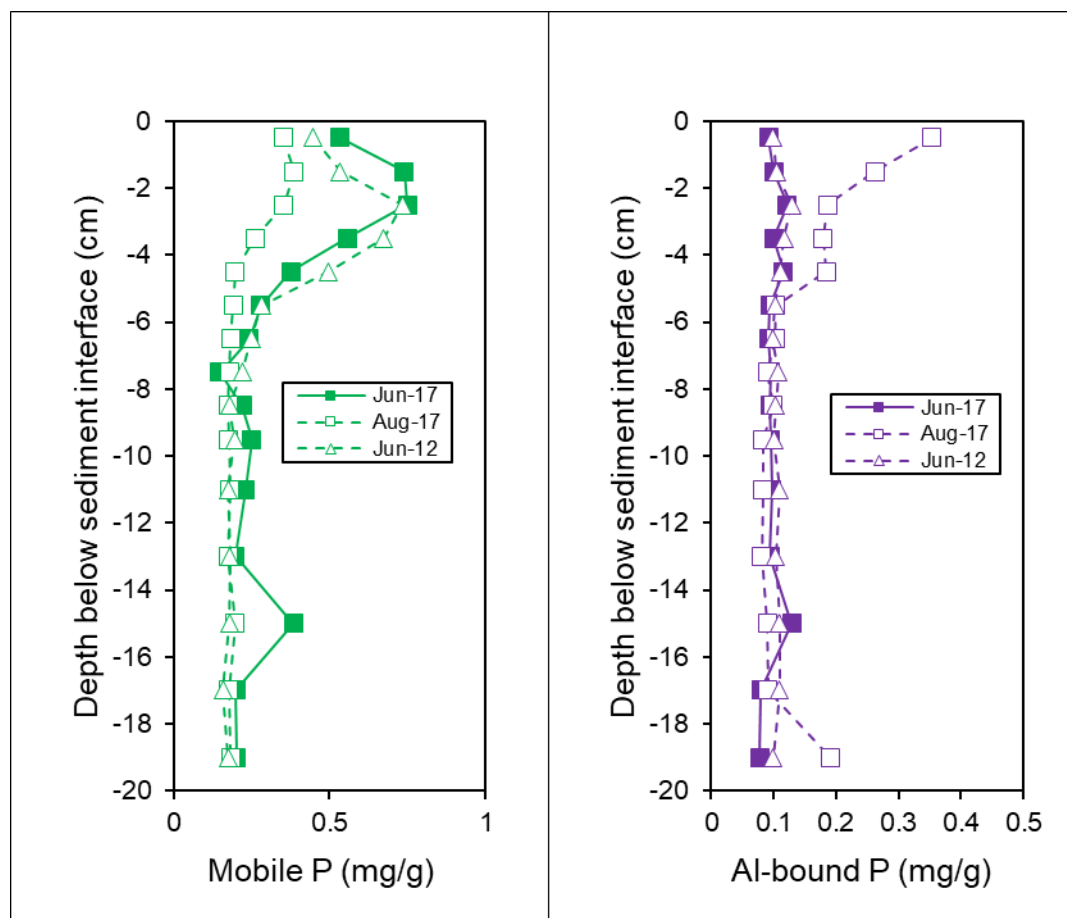


Figure 24. Vertical variations in sediment mobile (i.e., the sum of the loosely-bound P and iron-bound P sediment fractions) phosphorus (P) concentrations (left) and aluminum (Al)-bound P concentrations for a sediment core collected from station 2 (Figure 1) in June 2012, June 2017, and August 2017. The sediment profile in June of 2012 and 2017 represent pre-treatment conditions while August 2017 represents post-alum treatment conditions.

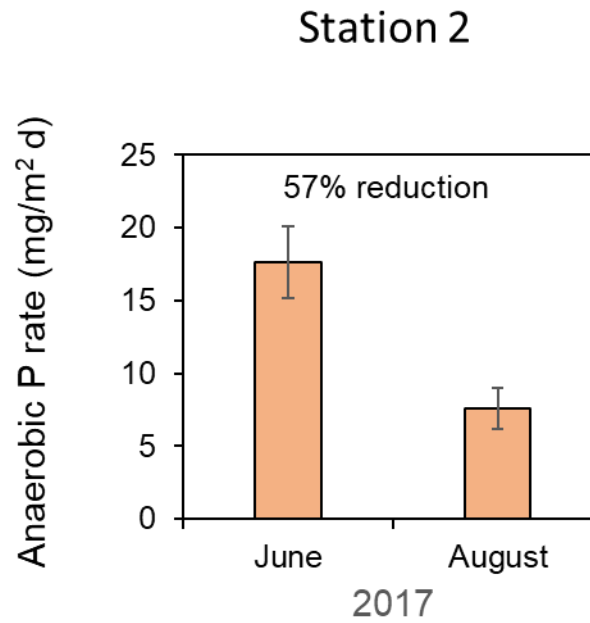


Figure 25. A comparison of mean ($n = 3$, see Figure 1) rates of diffusive phosphorus (P) flux from sediment under anaerobic conditions measured from sediment cores collected at station 2 in 2012 and 2017. Horizontal lines represent ± 1 standard error.